Detection of tibial fractures in cats and dogs with deep learning

Berker BAYDAN[1,a,✉], Halil Murat ÜNVER[1,b]

[1]Kırıkkale Üniversitesi, Mühendislik Fakültesi, Bilgisayar Mühendisliği Bölümü, Kırıkkale, TÜRKİYE
[a]ORCID: 0000-0003-2806-368X; [b]ORCID: 0000-0001-9959-8425

✉Corresponding author: baydanberker@gmail.com
Received date: 21.07.2020 - Accepted date: 21.12.2020

Abstract: The aim of this study is to classify tibia (fracture/no fracture) on whole/partial body digital images of cats and dogs, and to localize the fracture on fracture tibia by using deep learning methods. This study provides to diagnose fracture on tibia more accurately, quickly and safe for clinicians. In this study, a total of 1488 dog and cat images that were obtained from universities and institutions were used. Three different studies were implemented to detect fracture tibia. In the first phase of the first study, tibia was classified automatically as fracture or no fracture with Mask R-CNN. In the second phase, the fracture location in the fracture tibia image that obtained from the first phase was localized with Mask R-CNN. In the second study, the fracture location was directly localized with Mask R-CNN. In the third study, fracture location in the fracture tibia that obtained from the first phase of first study was localized with SSD. The accuracy and F1 score values in first phase of first study were 74% and 85%, respectively and F1 score value in second phase of first study was 84.5%. The accuracy and F1 score of second study were 52.1% and 68.5%, respectively. The F1 score of third study was 46.2%. The results of the research showed that the first study was promising for detection of fractures in the tibia and the dissemination of the fracture diagnosis with the help of such smart systems would also be beneficial for animal welfare.

Keywords: Cat, deep learning, dog, fracture, tibia.

Derin öğrenme ile kedi ve köpeklerde tibia kırıklarının tespiti

Özet: Bu çalışmanın amacı derin öğrenme yöntemleri kullanarak kedilerin ve köpeklerin bütün/kısmi dijital görüntüleri üzerinde tibiayı (kırık/kırık değil) sınıflandırmak ve kırık olarak tespit edilmiş tibialar üzerinde kırığın yerini lokalize etmektir. Bu çalışma klinisyenler için tibiadaki kırığın daha doğru, hızlı ve güvenli bir şekilde teşhis edilmesini sağlar. Bu araştırmada üniversitelerden ve kurumlardan sağlanan toplam 1488 adet köpek ve kedi görüntüsü kullanıldı. Tibia kırığı tespiti için üç farklı çalışma yapıldı. İlk çalışmanın ilk fazında, Mask R-CNN ile otomatik şekilde kırık ve sağlam tibia sınıflandırılması yapıldı. İkinci fazda ilk fazdan elde edilen kırık tibiadaki kırık yeri Mask R-CNN ile lokalize edildi. İkinci çalışmada, Mask R-CNN ile kırığın yeri doğrudan lokalize edildi. Üçüncü çalışmada SSD ile birinci çalışmanın birinci fazından elde edilen kırık tibiadaki kırık yeri lokalize edildi. İlk çalışmanın ilk faz doğruluk ve F1 skor değerleri sırasıyla %74 ve %85, birinci çalışmanın ikinci faz F1 skor değeri ise %84,5 olarak bulundu. İkinci çalışmanın doğruluk ve F1 skor değerleri sırasıyla %52,1 ve %68,5 olarak bulundu. Üçüncü çalışmanın F1 skor değeri ise %46,2 olarak bulundu. Araştırma sonuçları, ilk çalışmanın tibiada kırık tespiti için umut verici olduğunu ve bu tip akıllı sistemler yardımıyla kırık teşhisinin yaygınlaştırılmasının hayvan refahı yönünden de yararlı olacağını gösterdi.

Anahtar sözcükler: Derin öğrenme, kedi, kırık, köpek, tibia.

Introduction

Tibial fractures are common in dogs and cats (4). Tibiofibular and pelvic bone fractures were most common in dogs, pelvic limb fractures were most common in cats (1). Treatment of fractures is important. If the correct intervention is not performed, there may be complications in the fracture improvement process. So, it is essential to make a correct and quick decision (4). In general, x-ray images are used in the diagnosis of fracture in veterinary medicine. But, the diagnosis of bone fracture by taking X-Ray image is risky for clinicians due to radiation exposure.

It is also a costly and error-prone method in diagnosis (9). Sometimes, it may be difficult to diagnose a fracture or fracture type due to the low quality of the x-ray image or fatigue cause of demanding workloads for the general orthopedist or even the expert orthopedist (2, 3, 7, 10). These adverse conditions can be minimized by using deep learning technology. Rapid diagnosis and reporting are as important as an accurate diagnosis. The quick procedure will prevent patient harm due to delayed or missed diagnosis. (11).

X-ray images are frequently degraded by Poisson noise, which degrades the visual quality of the image and obscures important information required for an accurate diagnosis. Including a denoising step in automatic fracture detection process was used by several researchers (13). There are different methods for fracture detection based on X-ray and CT images. Some of them are Active contour model (ACM and GACM), Wavelet and Curvelet, Haar, Support Vector Machine (SVM) classifier, X-Ray/CT auto classification of fracture (GLCM), Novel morphological gradient based edge detection technique, Daubechies Wavelet and Fuzzy C-Means (FCM) Clustering, Using Classifiers DT, BN, NB, NN and mixed, Fusion Classification technique, Wavelet and Haar, Combined snake and GVF, Novel approach using binary tree and cuttoff, Using Discrete Wavelet Transform and ring, Using Bi Plane Slicing, Supervised learning based classification (10). Although there are many retrospective studies about the automatic determination of human bone fractures, no many studies have been found on animal fractures. There is a retrospective study only to evaluate the prevalence of appendicular fractures in dogs and cats in Libya (1). But this study does not relate to the automatic determination of bone fracture in animals by computer aided.

The aim of this study is to develop computerized system for classification of dog and cat tibia images whether fracture or no fracture and localization of the location of the fracture with Mask R-CNN and SSD which are the deep learning methods.

Materials and Methods

Dataset: In this study, the dataset was created from scratch. No fracture and fracture tibia images were collected from veterinary faculties and Ankara municipality. In order to get these images, contacted with Surgery Department of Veterinary Faculties of Ankara, Kırıkkale, and Selçuk Universities. Also, most of the images were supplied from Ankara Metropolitan Municipality Sincan Temporary Animal Care Home Rehabilitation Center. A total of 1488 dogs and cats whole/partial body images were selected among thousands of images. These 1488 images consisted of 988 dogs and 500 cats. These images were obtained in Digital Imaging and Communication in Medicine (DICOM) format. The anatomical structures of the dog and cat tibia are almost similar (5). Therefore, there is no difference between them in terms of detecting cat and dog fracture tibia.

Annotation of no fracture, fracture tibia and fracture location of fracture tibia: 1488 tibia images were annotated by a veterinarian. These images consisted of no fracture and fracture tibia. LabelImg (19) is a graphical image annotation tool for labeling image with bounding box. In order to annotate tibia images by using labelImg, 1488 DICOM images were converted to JPEG format. The Angora Viewer software installed on the institution's computer was used to convert DICOM to JPEG.

System architecture: The backbone of deep learning bases on neural networks. The architecture of deep learning that consists of many hidden layers and neurons, provides an advantage to obtain good results on coarse data or image as regards standard neural network (16). There are many deep learning technologies such as Mask R-CNN (6) and SSD (12). Mask R-CNN is a method that allows to detect objects in an image by localizing and masking. Mask R-CNN is the addition of the mask object in parallel with the existing bounding box identifier of Faster R-CNN. In the structure of Mask R-CNN, masks are implemented on each Region of Interest (ROI) to predict segmented part of object. It enables useful framework for implementation and training. Also, it provides fast framework (6). SSD is a deep learning algorithm that generates bounding boxes and their confidence score to detect objects on image and after that non-max suppression is applied on bounding box in order to achieve last detection (12).

Three different studies (S1, S2 and S3) were performed in order to detect, classify tibia and localize fracture location of fracture tibia. S1 is related to detect and localize fracture location of fracture tibia which is obtained automatically by system from whole/partial body digital image by using Mask R-CNN. S1 builds up two stages (Stage 1 and Stage 2). No fracture and fracture tibia were detected and classified by using Mask R-CNN in the first stage. After fracture tibia image was seperated automatically by system from whole/partial body digital image, fracture location was detected and localized by using Mask R-CNN on fracture tibia in the second stage. S2 is related to detect and localize fracture location of fracture tibia directly from whole/partial body digital image by using Mask R-CNN. Mask R-CNN architecture was used in this study (Figure 1). In S3, the SSD algorithm was used instead of the Mask R-CNN that is used in S1-Stage2 to localize the fracture location of fracture tibia which is obtained from S1-Stage1. SSD architecture was shown in Figure 1.

Proposed framework: According to performed studies, S1 is proposed. The flowchart of the proposed framework was shown in Figure 2. The proposed framework works fully automatic in all steps and stages. There is no manual process in the proposed framework. Therefore, this system proposed offers faster, more intelligent and accurate solution for fracture detection on tibia.
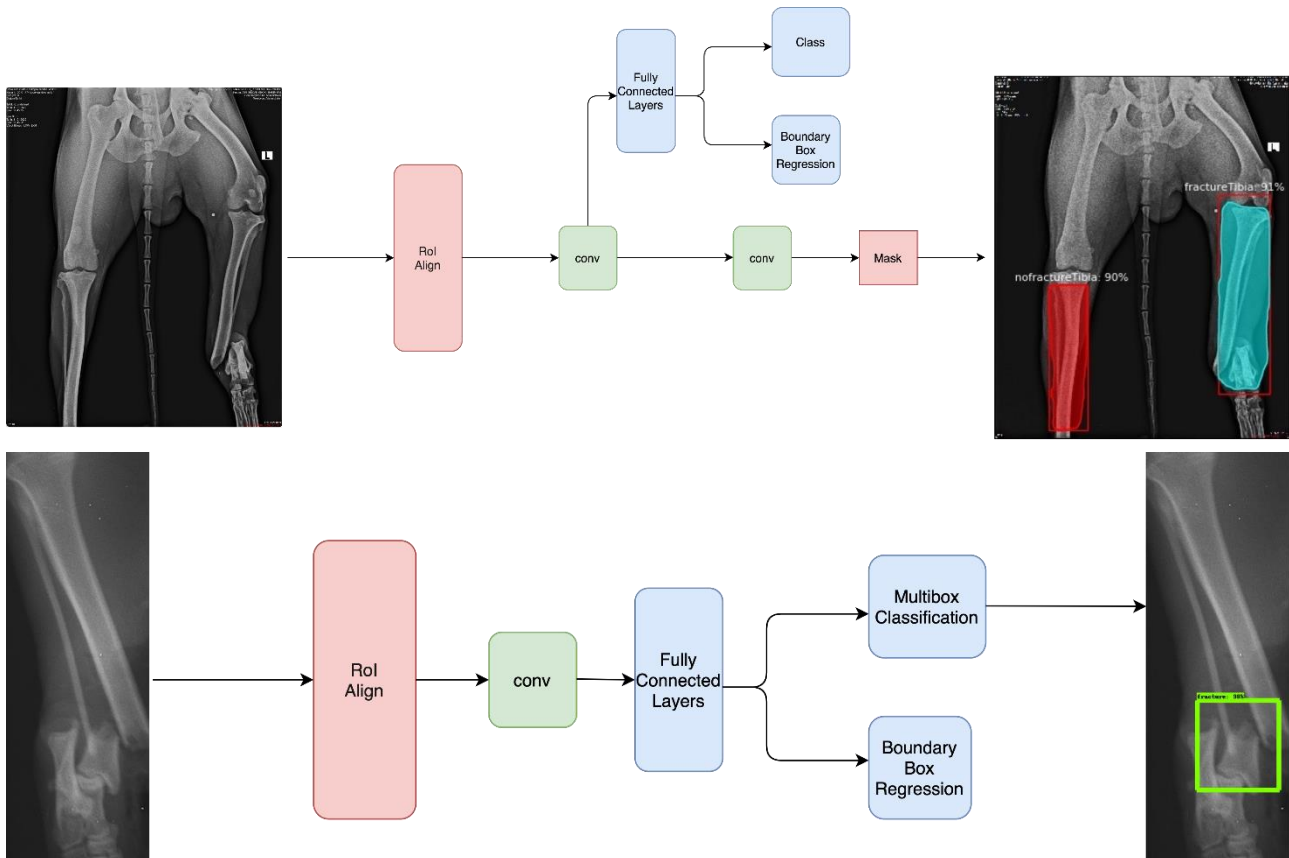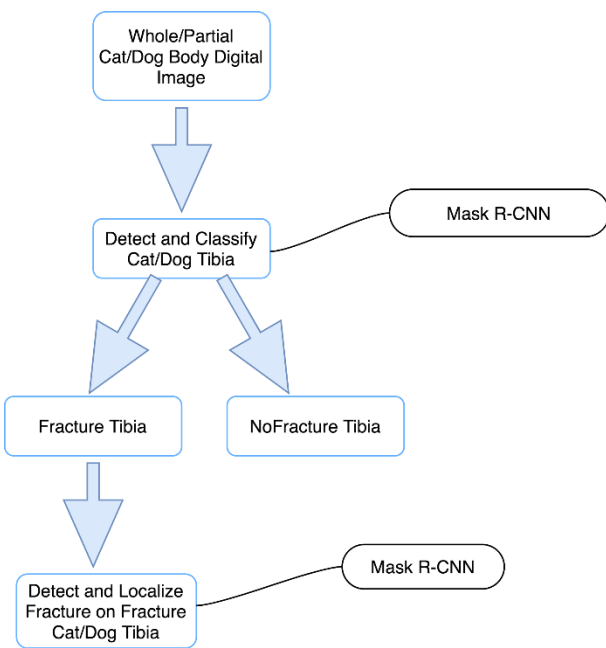
Figure 1. Mask R-CNN and SSD architecture.

Figure 2. The flowchart illustrating the proposed framework.

Training phase: Tibia dataset was trained by using Mask R-CNN for detection and classification of tibia and detection and localization fracture location of fracture tibia. The dataset consisted of two parts. First part was training and second part was testing. This dataset was re-trained with pre-trained Mask R-CNN model for the detection and localization of no fracture, fracture tibia and fracture location of fracture tibia. Thus, transfer learning process was generated for these studies. The weights of Mask_RCNN_COCO model were used for training. The configuration values of Mask R-CNN were specified during training phase. Batch size: 2, learning rate: 0.001, learning momentum: 0.9, weight decay: 0.0001, epoch: 4000. In order to perform different size of images, image was resized for scaling ratio in Mask R-CNN. Image_min_dim and image_max_dim was set to 800 and 1024 pixel, respectively. Images were scaled that small side was image_min_dim, but scaling doesn't applied if long side is greater than image_max_dim. The system was developed for S1 and S2 by using Keras API. Also, fracture tibia dataset that obtained from first phase of S1 was trained by using SSD for localization fracture on fracture tibia. The configuration values of SSD were specified during training phase. Batch size: 16, learning rate: 0.01, learning momentum: 0.9, weight decay: 0.9, epoch: 4000. Fixed shape resizer was used for scaling different size of images in SSD. Height and width was set to 300 and 300, respectively. The system was developed for S3 by using Tensorflow API. The implementations of these studies were performed on 30.5 GB NVIDIA Tesla M60 GPU and Ubuntu 18.04 operating system.

***Performance evaluation metrics*:** In order to evaluate performance of detection and classification of

tibia and detection and localization of fracture location of fracture tibia, some metrics have to be calculated. Intersection of Union (IoU) is required metric for evaluate performance of system. IoU is part that intersects between the ground truth and the bounding box on the image (18). When the ground truth and bounding box are compared, it is decided on whether the result is True Positive or False Positive through IoU. In this context threshold has to be determined for IoU. IoU was taken as 0.4 for S1, S2 and S3. For instance, if IoU is greater than 0.4, the result is True Positive. Otherwise, it is False Positive. The threshold for the IoU was determined by observing how accurately all the test data cover the fracture between ground truth and the bounding box found by the system. The IoU threshold for the detection of no fracture and fracture tibia and detection of fracture location directly from whole/partial body image was also determined by same method. Confidence score is important metric to evaluate system performance. Confidence score is the probability of detection fracture on fracture tibia or classification of tibia. If the annotated fracture overlaps the location detected as fracture by the system, it is called "True Positive-TP". If the annotated fracture does not overlap the location detected as fracture by system, it is called "False Positive-FP". If the system doesn't detect anything on the image but there is a fracture on the image, it is called "False Negative-FN". If there is no fracture on tibia and system also define "there is no fracture on tibia", it is called "True Negative-TN".

There can be multiple TP and FP on fracture tibia image. Let's assume highest confidence score is TP and second highest confidence score is FP. In this case, since the highest value is TP and it correctly detects the tibia fracture, only the value TP is used to measure the performance of the system. Therefore, FP is not used to calculate system performance. Let's say highest confidence score is FP and second highest confidence score is TP. In this case, both TP and FP are used to calculate system performance. The reason why the TP value is taken here is the correct detection of the tibia fracture with the second highest probability. Accuracy (15) is calculated for how system detect accurately. Accuracy is the ratio of cases that are True Positive and True Negative to all cases. In the light of these obtained metrics, F-Score (17) is calculated to determine the overall performance of the system.

Results

In the first stage of S1, 1488 no fracture and fracture tibia dataset were used. Total dataset was seperated as 595 no fracture and 595 fracture tibia images for training, 149 no fracture and 149 fracture tibia images for test. Dog dataset was seperated as 286 no fracture and 514 fracture

tibia images for training, 76 no fracture and 112 fracture tibia images for test. Cat dataset was seperated as 309 no fracture and 81 fracture tibia images for training, 73 no fracture and 37 fracture tibia images for test. Mask R-CNN was used to detect and classify no fracture and fracture tibia from whole/partial body image. IoU rate was specified as greater than 0.4. The accuracy and F1 score of model on the total dataset were 74% and 85% respectively. Only 7 images out of 149 could not make a prediction for the classification of fracture tibia. Only 2 images out of 149 were unable to make a prediction for classification of no fracture tibia. The accuracy and F1 score of model on the dog dataset were 72.4% and 84% respectively. Only 2 images out of 112 could not make a prediction for the classification of fracture tibia. Only 1 images out of 76 were unable to make a prediction for classification of no fracture tibia. The accuracy and F1 score of model on the cat dataset were 76.6% and 86.7% respectively. Only 1 images out of 37 could not make a prediction for the classification of fracture tibia. Only 1 image out of 73 were unable to make a prediction for classification of no fracture tibia. Thus, 518 fracture tibia (441 dog and 77 cat) images were detected automatically by system from 744 fracture tibia (626 dog and 118 cat fracture tibia) images. 744 fracture tibia images consisted of training and testing sets. 518 fracture tibia images obtained as a result of training and testing were automatically extracted from the whole/partial body image by the coordinates of the bounding box. The detected and classified no fracture and fracture tibia from a whole body image was shown in Figure 3.

No fracture and fracture tibia in 298 total test data were detected and classified within 433.1 seconds. It took an average of 1.45 seconds for an image. No fracture and fracture tibia in 188 dog test data were detected and classified within 272.6 seconds. No fracture and fracture tibia in 110 cat test data were detected and classified within 159.5 seconds. In second stage of S1, a total of 518 fracture tibia were divided into 415 training (360 dog and 55 cat) and 103 test (81 dog and 22 cat) data on the images of the fracture tibia. IoU rate was specified as greater than 0.4. The F1 score of model on the total dataset was 84.5%. Only 8 images out of 103 could not make a prediction for the detection of fracture on the fracture tibia. The F1 score of model on the dog dataset was 87.1%. Only 6 images out of 81 could not make a prediction for the detection of fracture on the fracture tibia. The F1 score of model on the cat dataset was 74.3%. Only 2 images out of 22 could not make a prediction for the detection of fracture on the fracture tibia. The detected fracture location on fracture tibia which was obtained automatically by system from whole/partial body image by using Mask R-CNN was shown in Figure 4.
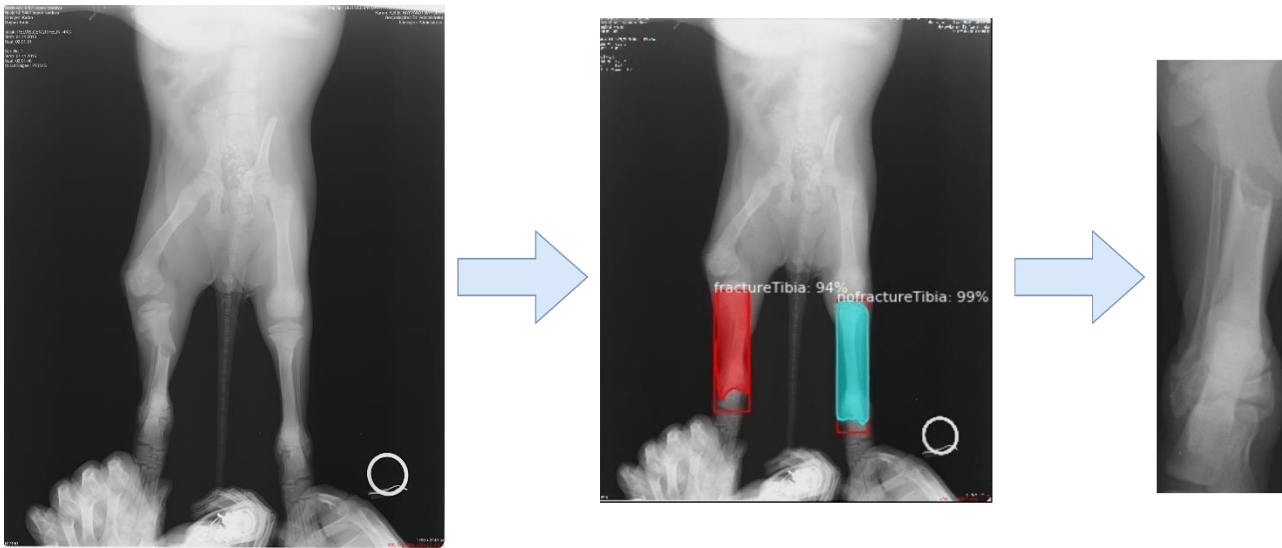
Figure 3. The detected and classified nofracture and fracture tibia from whole body image by using Mask R-CNN.
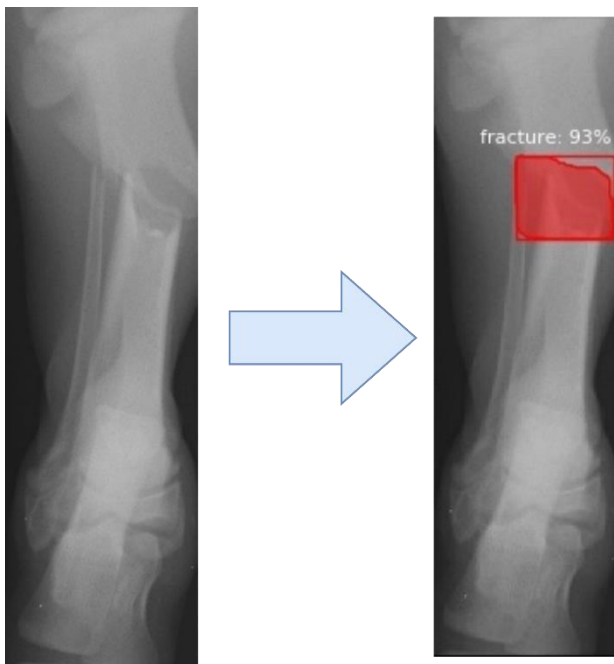

Figure 4. The detected fracture location on fracture tibia which was obtained automatically by system from whole/partial body image by using Mask R-CNN.

Fracture location of fracture tibia in 103 test data were detected and localized within 375.3 seconds. It took an average of 3.6 seconds for an image. Fracture location of fracture tibia in 81 dog test data were detected and localized within 291.6 seconds. Fracture location of fracture tibia in 22 cat test data were detected and localized within 79.2 seconds. The full cycle composed of two stages. No fracture and fracture tibia were detected and classified by using Mask R-CNN in the first stage and fracture location of fracture tibia which was obtained automatically by system from whole/partial body images by using Mask R-CNN was detected and localized in the second stage. The full cycle of automatic fracture detection by system on fracture tibia took an average of 5.05 seconds for an image.

In S2, 744 images containing total dataset fracture tibia were seperated as 595 training data and 149 test data. 149 test data were used as no fracture tibia. Dog dataset was seperated as 514 training data and 112 test data. 76 dog test data were used as no fracture tibia. Cat dataset was seperated as 81 training data and 37 test data. 73 cat test data were used as no fracture tibia. IoU rate was specified as greater than 0.4. The accuracy and F1 score of model on the total dataset were 52.1% and 68.5% respectively. Only 35 images out of 149 could not make a prediction for the detection of fracture location of fracture tibia directly from whole/partial body. The accuracy and F1 score of model on the dog dataset were 51.7% and 68.1% respectively. Only 28 images out of 112 could not make a prediction for the detection of fracture location of fracture tibia directly from whole/partial body. The accuracy and F1 score of model on the cat dataset were 53% and 69.3% respectively. Only 7 images out of 37 could not make a prediction for the detection of fracture location of fracture tibia directly from whole/partial body. The detected and localized fracture location of fracture tibia directly from whole/partial body image by using Mask R-CNN was shown in Figure 5.

Fracture location of fracture tibia directly from whole/partial body images in 149 test data were detected and localized within 2991.8 seconds. It took an average of 20 seconds for an image. Fracture location of fracture tibia directly from whole/partial body images in 112 dog test data were detected and localized within 2520 seconds. Fracture location of fracture tibia directly from whole/partial body images in 37 cat test data were detected and localized within 460 seconds.
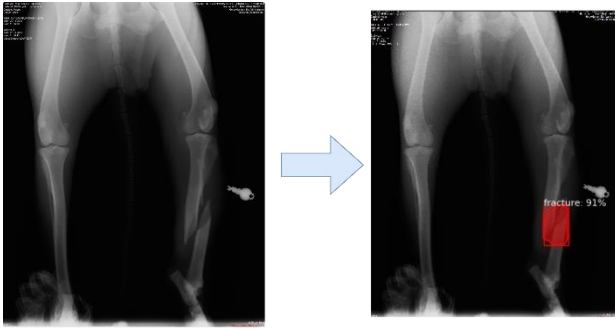
Figure 5. The detected and localized fracture location of fracture tibia directly from whole/partial body image by using Mask R-CNN.
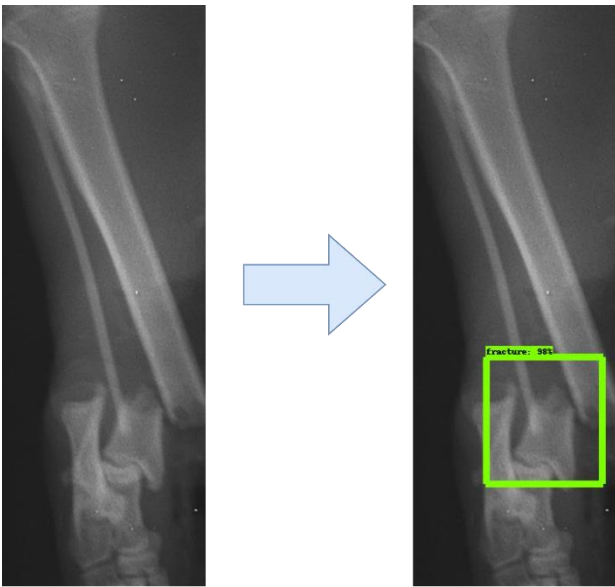

Figure 6. The detected fracture location on fracture tibia which was obtained automatically by system from whole/partial body image by using SSD.

Table 1. Detection, classification and localization studies of fracture in tibia using Mask R-CNN.

| Studies (S) | Mask R-CNN | | | | | | | | | | | | | | | | | | | | |
| | **Dog** | | | | | | | **Cat** | | | | | | | **Total** | | | | | | |
	P (%)	R (%)	A (%)	Se (%)	Sp (%)	F1 (%)	ART (sec)	P (%)	R (%)	A (%)	Se (%)	Sp (%)	F1 (%)	ART (sec)	P (%)	R (%)	A (%)	Se (%)	Sp (%)	F1 (%)	ART (sec)
S1-St1	74.5	96.2	72.4	92.4	84.8	84	1.45	77.6	98.3	76.6	94.4	89.3	86.7	1.45	75.7	97	74	92.7	86.9	85	1.45
S1-St2	83.1	91.4	-	-	-	87.1	3.6	65	86.6	-	-	-	74.3	3.6	79.3	90.5	-	-	-	84.5	3.6
S2	59.6	79.5	51.7	73.2	40.7	68.1	20	57.7	86.6	53	61.9	53.4	69.3	20	59	81.7	52.1	71.3	46.9	68.5	20

P: Precision   R: Recall   A: Accuracy   Se: Sensitivity   Sp: Specificity   F1: F1 Score   ART: Average Response Time.

In S3, fractures on fracture tibia were detected using SSD deep learning algorithm instead of Mask R-CNN as in the second phase of S1. IoU rate was specified as greater than 0.4. The F1 score of model on the total dataset were 46.2%. Only 36 images out of 103 could not make a prediction for the detection of fracture on the fracture tibia. The F1 score of model on the dog dataset was 48.1%. Only 26 images out of 81 could not make a prediction for the detection of fracture on the fracture tibia. The F1 score of model on the cat dataset was 42.9%. Only 10 images out of 22 could not make a prediction for the detection of fracture on the fracture tibia. The detected fracture location on fracture tibia which was obtained automatically by system from whole/partial body image by using SSD was shown in Figure 6.

Fracture location of fracture tibia in 103 test data were detected and localized within 7.8 seconds. It took an average of 0.075 seconds for an image. Fracture location of fracture tibia in 81 dog test data were detected and localized within 6.15 seconds. Fracture location of fracture tibia in 22 cat test data were detected and localized within 1.575 seconds. The metrics of these studies were given in Table 1 and 2.

Table 2. Fracture detection on tibia using SSD.

Study (S)	SSD																				
	Dog							Cat							Total						
	P (%)	R (%)	A (%)	Se (%)	Sp (%)	F1 (%)	ART (sec)	P (%)	R (%)	A (%)	Se (%)	Sp (%)	F1 (%)	ART (sec)	P (%)	R (%)	A (%)	Se (%)	Sp (%)	F1 (%)	ART (sec)
S3	46.4	50	-	-	-	48.1	0.075	50	37.5	-	-	-	42.9	0.075	46.2	46.2	-	-	-	46.2	0.075

P: Precision   R: Recall   A: Accuracy   Se: Sensitivity   Sp: Specificity   F1: F1 Score   ART: Average Response Time.

Discussion and Conclusion

Automatic fracture detection system is remarkable subject in diagnosis of fracture. There are many studies performed in human fracture. However, there are not many studies in animals regarding automatic fracture detection system using deep learning method. This is the first automatic fracture detection smart system on dogs and cats. In current research, no preprocess and data augmentation methods were applied. According to test results, tibia fracture detection performance of the proposed framework which was related to combination of first stage and second stage of S1 (84.5%) was higher than tibia fracture detection performance of S2 (68.5%) and S3 (46.2%). Also, the response time of proposed framework (5.05 seconds) was faster than the response time of S2 (20 seconds). Although the performance of the S3 was the lowest, the response time was obtained to be faster than the S1 and the S2. When the dog and cat dataset were evaluated separately using both Mask R-CNN and SSD in all studies, it was observed that the performance of the detection of fracture location of fracture tibia in dog was higher than in cats (Table 1 and 2). The reason for this may be that the number of cats in total dataset is less than the number of dogs. In various human clinical studies involving computer-aided fracture detection had been found different performance (metric) values (8). In some of these research by using radiographs as modality, accuracy, sensitivity and specificity were found as 0.83 (14), 0.90 and 0.88 (11), respectively for Wrist/Hand/Ankle. In the study of proximal humerus by Chung et al., accuracy, sensitivity and specificity for detection were found as 0.96, 0.99 and 0.97, respectively. According to results of S1 of this research, accuracy was less than the result of previous some researches, but sensitivity and specificity were similar (Table 1). On the other hand, the detection performance (F1-score) of fracture location on the fracture tibia in this research was high 84.5%. The low accuracy in this study may be due to the fact that the digital images used belong to very different dog and cat breeds and the difference in the method used.

The most important aspect of this study compared to the other researches (i.e fracture detection on proximal humerus which is cropped manually from radiograph (2)) was to detect fracture tibia automatically from whole/partial body image and then localize fracture location automatically on fracture tibia.

As far as the result of proposed system, the metrics were promising regarding to detect and localize fracture on tibia of cats and dogs. The dissemination of the fracture diagnosis with the help of such smart systems would also be beneficial for animal welfare.

Ethical Statement

This study was approved by the Kırıkkale University Animal Experiments Local Ethics Committee (60821397-010.99).

Conflict of Interest

The authors declared that there is no conflict of interest.

References

1. **Bennour EM, Abushhiwa MA, Ben Ali L, et al** (2014): *A retrospective study on appendicular fractures in dogs and cats in Tripoli – Libya.* J Vet Adv, **4**, 425-431.
2. **Chung SW, Han SS, Lee JW, et al** (2018): *Automated detection and classification of the proximal humerus fracture by using deep learning algorithm.* Acta Orthop, **89**, 468-473.
3. **Eksi Z, Dandil E, Cakiroglu M** (2012): Computer aided bone fracture detection. In: 2012 20th Signal Processing and Communications Applications Conference (SIU). Muğla, Turkey.
4. **Glyde M, Arnett R** (2006): *Tibial fractures in the dog and cat: options for management.* Ir Vet J, **59**, 290-295.
5. **Hayashi K, Kapatkin AS** (2012): Fractures of the tibia and fibula, 999-1014. In: KM Tobias, SA Johnston (Eds), Veterinary Surgery Small Animal. Volume One, E-BOOK: 2-Volume Set, Elsevier Inc., Canada.
6. **He K, Hkioxari G, Dollar P et al** (2018): Mask R-CNN. 2980-2988. In: IEEE International Conference on Computer Vision (ICCV). Venice, Italy. arXiv:1703.06870v3 [cs.CV].
7. **Joshi D, Singh T** (2020): *A survey of fracture detection techniques in bone x-ray images.* Artif Intell Rev, **53**, 4475–4517.
8. **Kalmet PHS, Sanduleanu S, Primakov S et al** (2020): *Deep learning in fracture detection: a narrative review.* Acta Orthop, **91,** 215-220.

9. **Khan M, Sirdeshmukh, SPSMA, Javed K** (2016): Evaluation of Bone Fracture in Animal Model Using Bio-electrical Impedance Analysis. Perspectives in Science, **8**, 567-569.

10. **Khatik I** (2017): A *study of various bone fracture detection techniques.* Int J Eng Comput Sci, **6**, 21418-21423.

11. **Kim DH, MacKinnon T** (2017): *Artificial intelligence in fracture detection: transfer learning from deep convolutional neural networks*. Clin Radiol, **73**, 439-445.

12. **Liu W, Anguelov D, Erhan D et al** (2016): *SSD:* Single Shot MultiBox Detector. arXiv:1512.02325 [cs.CV]. Available at https://arxiv.org/pdf/1512.02325.pdf. (Accessed October 21, 2020).

13. **Mahendran SK, Santhosh Baboo S** (2011): *An enhanced tibia fracture detection tool using image processing and classification fusion techniques in x-ray images*. GJCST, **11**, 23-28.

14. **Olczak J, Fahlberg N, Maki A et al** (2017). *Artificial intelligence for analysing orthopaedic trauma radiographs.*

Acta Orthop, **88**, 581-586.

15. **Rani S, Kumari M, Amulya G et al** (2019): *Leg bone fracture segmentation and detection using advanced morphplogical techniques.* Int J Recent Technol Eng, **8**, 1246-1249.

16. **Ravi D, Wong C, Deligianni F et al** (2017): *Deep Learning for Health Informatics.* IEEE J Biomed Health, **21**, 4-21.

17. **Tsuruoka Y, Tsujii J** (2003): Boosting precision and recall of dictionary-based protein name recognition. 41-48. In: Proceedings of the ACL 2003 workshop on Natural language processing in biomedicine. Sapporo, Japan.

18. **Tychsen-Smith L, Petersson L** (2018): Improving object localization with fitness nms and bounded IOU loss. arXiv:1711.00164v3 [cs.CV]. Available at https://arxiv.org/pdf/1711.00164.pdf. (Accessed July 21, 2020).

19. **Tzutalin** (2015): LabelImg. Git code. Available at https://github.com/tzutalin/labelImg. (Accessed February 27, 2020).